2017 IEEE International Conference on Advanced Intelligent Mechatronics (AIM)
Sheraton Arabella Park Hotel, Munich, Germany, July 3-7, 2017

Development of an air duct cleaning robot for housing based on peristaltic crawling motion

Y. Tanise, K. Taniguchi, S. Yamazaki, M. Kamata, Y. Yamada, *Member, IEEE*, and T. Nakamura, *Member, IEEE*

***Abstract*—In recent years, ventilation equipment has been installed in various structures to draw in outdoor air and circulate indoor air. These ventilation installations have pipes (ducts) through which air flows. If dust accumulates in a duct, it will be carried indoors by the airflow. Dust adversely affects human health, and so these ducts must be cleaned regularly. However, the existing cleaning methods are inadequate for the Ducts having small diameter and many curved points, that are used in houses. Thus, to clean such ducts, we have developed a robot that moves imitating peristaltic crawling. This motion is suitable for moving in ducts because it is stable in curved and narrow pipes. In addition, the robot can move and clean the duct at the same time because it moves forward by holding the pipe walls. In this paper, we outline the development of such a robot. From the results of using the robot to clean the inside of duct, we find a cleaning performance of it.**

I. Introduction

In recent years, ventilation installations have been installed in various structures (e.g., buildings, factories, and houses) to draw in outdoor air and circulate indoor air. As shown in Fig. 1, these ventilation installations comprise pipes (known as ducts) through which air flows. If dust accumulates in a duct, it will be carried indoors by the airflow. Because dust adversely affects human health, the ducts must be cleaned regularly [1] [2].

Existing cleaning methods involve the use of a self-propelled robot or a cleaning tool driven by air pressure [3]–[5]. An operator inserts the cleaning device in one end of the duct, and the dust is collected at the other end. This method is suitable for the relatively wide and straight ducts that are used in buildings and factories. However, it is inadequate for the narrower and more curved ducts that are used in houses. Therefore, a method is required to clean such housing ducts.

We have developed a robot that can clean housing ducts. The specifications of the targeted duct are as follows: an inner diameter of 75 mm, a minimum radius of curvature of 70 mm, and a length of 10 m. These are commonly used sizes (see Fig. 3). First, we focus on a motion method of the robot. There are several motion patterns for robots traveling in pipes, e.g., snake-type [6], wheel-type [7], and ciliary vibration-type [8]. However, snake-type and wheel-type robots are not suitable for traveling in narrow pipes, and ciliary vibration-type robots cannot travel backward or climb vertical pipes. Thus, we need a different method of locomotion that is suitable for traveling in ducts. In addition, it is necessary to scrape off the dust while cleaning the duct because some of the dust adheres to the inner duct wall. Hence, we chose to focus on the peristaltic crawling of an earthworm. This type of locomotion is suitable for narrow curved ducts because it requires only a small space for the robot moves and has a large contact area against the inner duct. Additionally, imitating such motion with a cleaning part attached to the area in contact with the duct wall would scrape off the dust because an earthworm moves forward while holding the surrounded walls.

Therefore, in this paper, we develop a cleaning unit and measure its characteristics and clearance. We then measure the clearance of the robot with the cleaning unit attached, and assess its effectiveness.

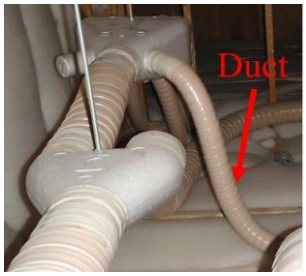

Figure 1. Appearance of a duct

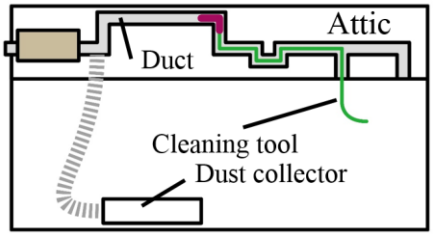

Figure 2. Existing cleaning method

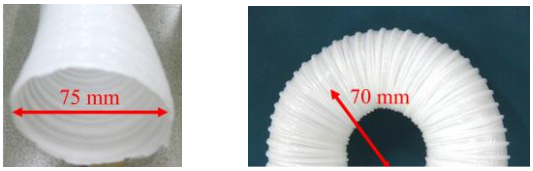

(a) Front view (b) Curved point view

Figure 3. Duct to be cleaned

Yuki Tanise, Kosuke Taniguchi, Shota Ymazaki, and Masashi Kamata are with the Department of Precision Mechanics, Faculty of Science and Engineering, Chuo University, 1-13-27 Kasuga, Bunkyo-ku, Tokyo 112-8551, Japan (e-mail: t_tomita@bio.mech.chuo-u.ac.jp).

Yasuyuki Yamada and Taro Nakamura are with the Department of Precision Mechanics, Faculty of Science and Engineering, Chuo University, 1-13-27 Kasuga, Bunkyo-ku, Tokyo 112-8551, Japan (e-mail: nakamura@mech.chuo-u.ac.jp).

II. Peristaltic Crawling of an Earthworm

Peristaltic crawling is the motion by which earthworms and inchworms move forward. We develop a robot that imitates this motion.

An earthworm's body consists of 110–200 cylindrical segments, the inner structure of which is illustrated in Fig. 4(a). The earthworm has two muscle layers: a circular muscle arranged circumferentially inside the skin and a longitudinal muscle arranged inside the circular muscle in the axial direction. The former elongates the segments, and the latter contracts them in the axial direction. Figure 4(b) shows a flow of the contraction and expansion pattern in the earthworm's peristaltic crawling. Firstly, the earthworm uses its longitudinal muscles to contract its forward segments. This contraction is then transmitted successively to the rear segments. Simultaneously, the circular muscles elongate the forward segments, and the contracted segments generate a friction force between themselves and the surrounding surface. In turn, this friction force generates a reaction force that elongates the contracted segments. This repetitive contraction and extension generate longitudinal and backward waves by which the earthworm moves forward.

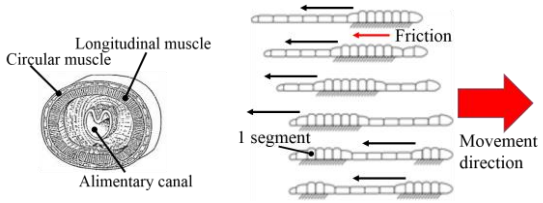

(a) Inner structure (b) Peristaltic crawling

Figure 4. Peristaltic crawling pattern of earthworm

III. Peristaltic Crawling Robot

A. Outline of peristaltic robot

Figure 5 shows the appearance of a developed peristaltic crawling robot. There are four units that are connected by three joints, and the robot travels by imitating the motion of an actual earthworm. Each unit performs the same function as a segment of an earthworm.

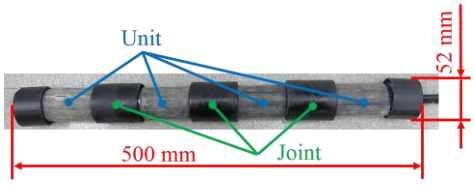

Figure 5. Peristaltic crawling robot

B. Unit

Figure 6 shows the structure of a unit. It consists of two flanges, bellows, a quick exhaust valve (EQU-6; PISCO), and a straight-fiber-type artificial muscle. The unit corresponds to actuation of the robot. When the air pressure is applied to inside the unit, the unit contracts axially and expands radially, as shown in Fig. 7. By sending this motion from the leading unit to the trailing one, waves of expansion and contraction are transmitted rear the body, causing the robot to move forward. Furthermore, installing a quick exhaust valve inside the unit reduces the exhaustion time. This is because the air in the unit is discharged not from the solenoid valve located 10 m away but from the unit directly (see Fig. 8).

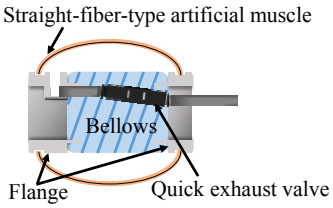

Figure 6. Structure of a unit

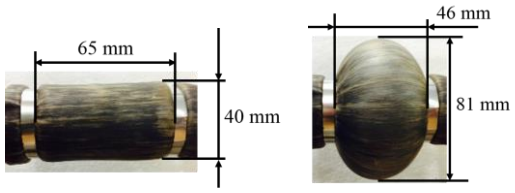

(a) Unpressurized (b) Pressurized

Figure 7. Appearance of a unit

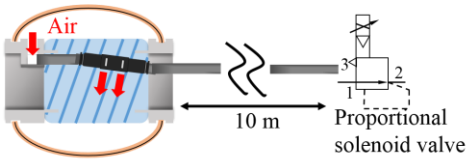

Figure 8. Exhausting the air from inside a unit

C. Joint

Figure 9 shows the appearance of a joint. By making joints to connect the units, it is possible to attach/detach them individually. As a result, the number and/or type of units can be changed to suit the surrounding environment, thereby helping to improve versatility. Making the joints wider than the units prevents the deflated artificial muscles (which have a higher static friction coefficient than that of the joints) from coming into contact with the duct, thereby reducing the overall frictional force.

(a) Top view (b) End view

Figure 9. Appearance of a joint

D. Control system

Figure 10 shows the control system that operates the robot. The robot is controlled by an Arduino Mega 2560 microcomputer. The D/A converter converts the digital output from the Arduino into an analog signal that is sent to a proportional solenoid valve. The air pressure supplied to the robot via a manifold from a compressor is proportional to the input voltage. Thus, the units are free to extend and contract independently.

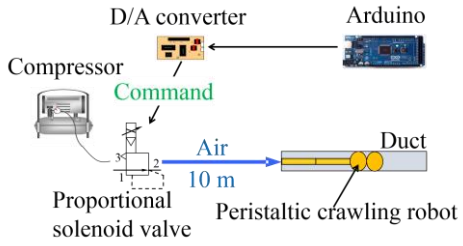

Figure 10 Control system of the peristaltic crawling robot

E. *Motion pattern*

By altering the extension/contraction combination of each unit, the robot can travel by several motion patterns. These are characterized by their wave-length (l), wavenumber (n), and number of propagations (s), which are defined as the number of units extended in the axial direction, the number of wavelengths in a bundle, and the number of units sent backward in one action, respectively, where N is the number of units. Hereinafter, the basic motion patterns are described as l–n–s; for example, motion 2–1–1 is shown in Fig. 11.

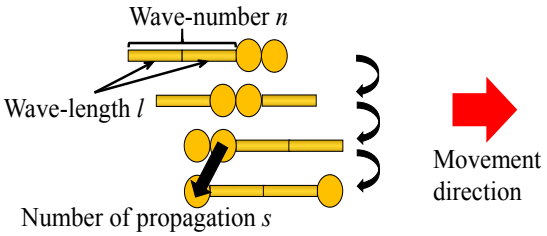

Figure 11 Motion pattern

IV. Cleaning Unit

A. *Suggested method of cleaning*

It is necessary to scrape off the dust in order to clean it because some of it adheres to the duct wall. We focus on using the peristaltic crawling motion itself to do this job. The robot travels by the repeated extension/contraction of the artificial muscles, which come into contact with the duct walls. Hence, attaching brushes to the exteriors of the artificial muscles would scrape off the dust when the artificial muscles contract, thereby avoiding the need for another actuator (see Fig. 12).

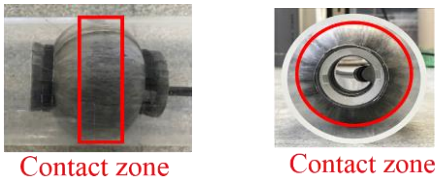

(a) Top view (b) End view

Figure 12. Artificial muscle pressing against duct walls

B. *Selecting a cleaning tool*

We use a brush to cleaning the duct, and conduct experiments with three types of brush that have different lengths and stiffness. Their respective efficacies are measured and compared in order to find the ideal cleaning characteristics. The first brush has an ultra-crimped pile (brush 1, Fig. 13), the second is a mop brush (brush 2, Fig. 14), and the third is a nylon brush (brush 3, Fig. 15). Table I lists the characteristics of the brushes.

Figure 13. Ultra-crimped pile

Figure 14. Mop brush

Figure 15. Nylon brush

TABLE I. FEATURES OF THE THREE BRUSH TYPES

	Length of tips of brush & Hardness
Ultra-crimped pile	7 mm & Soft
Mop brush	11 mm & Soft
Nylon brush	11 mm & Hard

C. *Cleaning unit*

Figure 16 shows the appearance of the developed cleaning units. Hereinafter, a unit equipped with brush 1, 2, or 3 is referred to as cleaning unit 1, 2, or 3, respectively. The brush should not disturb the expansion/contraction of its cleaning unit, so each brush was pasted on an aluminum sheet with axial cut-outs and wrapped around the unit with Velcro tape. As a result, when the cleaning unit contracts, the cuts of aluminum sheet expand. Therefore, expansion/contraction of the cleaning unit is not disturbed. In addition, the aluminum sheet has three separate cutouts to allow the artificial muscle to bulge out and come into contact with the duct.

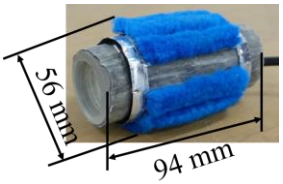

(a) Unit 1 (ultra-crimped)

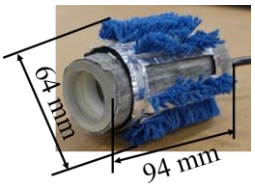

(b) Unit 2 (mop brush)

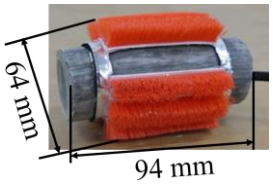

(c) Unit 3 (nylon brush)

Figure 16. Cleaning units

Figure 17. Aluminum sheet with brushes

V. Experiments to Assess Cleaning Characteristics

A. Measurement of maximum friction force

The maximum static frictional force when the cleaning unit holds the duct needs to exceed the traction force required for the robot to travel the target cleaning distance of 10 m. Since the result of measuring the required traction force was 72 N, we examine whether the maximum static frictional force of the cleaning unit exceeds 72 N.

Figure 18 shows the experimental arrangement. Firstly, the unit is connected to a load cell and placed in the acrylic pipe (inner diameter: 75 mm). Air pressure is then applied to the unit and the unit is pulled while it holds the pipe. The value measured at the moment the unit starts to move is taken as the maximum static frictional force of the cleaning unit. The applied pressure is raised in 0.01-MPa increments from 0.1 MPa.

Figure 19 shows the experimental results. The maximum static frictional force exceeded 72 N when 0.12 MPa was applied to cleaning unit 1, 0.14 MPa was applied to cleaning unit 2, and 0.15 MPa was applied to cleaning unit 3. However, this value is less than the maximum static frictional force of 180 N when 0.1 MPa is applied to the units without brushes. This is because the artificial muscle has a higher static friction coefficient than those of the brushes. By attaching a brush around the artificial muscle, the contact area of the latter with the pipe was reduced. The maximum static frictional forces of the cleaning units decreased from cleaning unit 1 to 2 to 3. The shorter and softer the brush, the larger the maximum static frictional force.

From these experimental results, the air pressure to be applied to the cleaning unit was determined as 0.15 MPa, at which the maximum static frictional force of all the cleaning units exceeds 72 N.

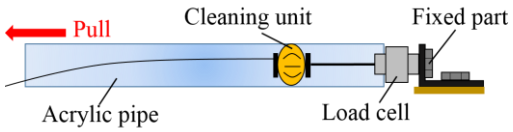

Figure 18. Experimental arrangement for measuring the maximum friction force

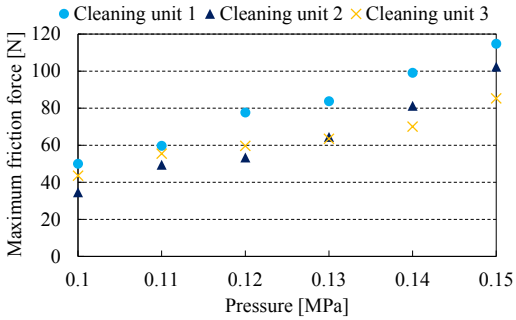

Figure 19. Maximum friction force

B. Characteristics of extension and contraction

In order to operate the robot, it is necessary to determine the operation cycle of the proportional solenoid valve used for pressure control. For this, it is necessary to measure the contraction and extension times of the cleaning unit.

Figure 20 shows the experimental arrangement. Firstly, the cleaning unit is connected to one end of the fixed end inside the duct and a slider is connected to the other. In this state, air pressure is applied to the cleaning unit, which expands and contracts. Here the applied pressure is 0.15 MPa, the tube length is 10 m, and the inner tube diameter is 4 mm.

Table II gives the experimental results. Compared with the unit without the brush, the contraction time of the cleaning unit increased and the amount of contraction decreased. The reasons are as follows. Firstly, the aluminum sheet to which the brush is attached restricted the contraction of the cleaning unit. Secondly, the artificial muscle's expansion diameter reduced due to the height of the brush. From these experimental results, the contraction and extension times of each unit were determined as 0.9 s and 0.6 s, respectively because all the cleaning units finished extension/contraction motion.

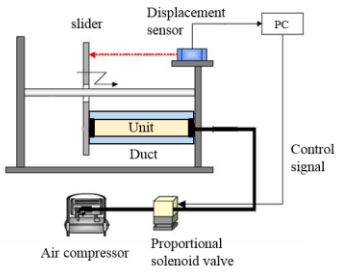

Figure 20. Experimental arrangement for measuring extension and contraction times

TABLE II. EXTENSION AND CONTRACTION RESPONSES

	Contraction time [s]	Extension time [s]	Amount of contraction [mm]
Non-pile	0.6	0.6	16
Unit 1	0.9	0.6	14
Unit 2	0.83	0.66	15.7
Unit 3	0.87	0.63	15.9

C. *Measurement of cleaning performance*

By measuring the cleaning performance of each developed cleaning unit, we can compare the effect of brush length and stiffness in cleaning. For this, only the leading unit of the robot is used a cleaning unit, and it travels inside the dirty pipe as shown in Fig. 21.

Figure 22 shows the experimental arrangement. The pressure is 0.15 MPa, the length of the air tubes is 10 m, the inner diameter of the air tubes is 4 mm, the contraction time is 0.9 s, and the extension time is 0.6 s. The inside of the acrylic pipe (inner diameter: 75 mm; weight: 461 g; length: 500 mm) is coated in test powder (silica sand) by the following method.

- The inside of the acrylic pipe is wetted with water.
- One end of the pipe is closed, and 50-g of test powder is put into the pipe and adheres to the whole duct uniformly.
- The inside of the pipe is wetted with water again.

We measure the amount of test powder before and after the robot cleans the pipe, from which we calculate the cleaning performance as a percentage using Eq. (1). Here, E is the cleaning performance, M is the weight of test powder before cleaning, and m is the weight of test powder after cleaning:

$$E = \left(\frac{M-m}{M}\right) \times 100 \ . \qquad (1)$$

Figures 23–26 show the appearance of the pipe after cleaning by the unit without brushes and by cleaning units 1, 2, and 3, respectively. Table III gives the diminution of test powder and the calculated cleaning performance. The best cleaning is with cleaning unit 3, followed in order by 2 then 1. Therefore, the stiffer and longer the brush, the better the cleaning. We consider the explanations to be 1) the stiffer the brush, the more test powder is dislodged, and 2) the longer the brush, the larger its contact area with the test powder. However, if the brush is too stiff and long, it could become difficult for it to pass through bends in the duct. Consequently, we choose moderate stiffness and length.

From these experiments, the maximum cleaning performance is 60.0%. However, the desirable residual amount of dust in the duct after cleaning is 1 g/m^2 or less, which equates to a cleaning performance of 99.8% in the case of this experimental environment. In order to improve the cleaning performance, we consider it necessary to increase the scraping off force

Figure 21. Appearance of the robot

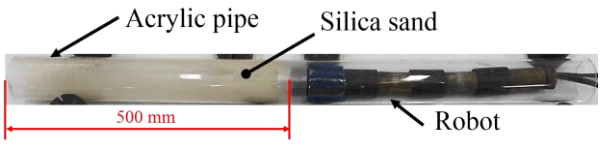

Figure 22. Experimental arrangement for cleaning the pipe using the cleaning units

Figure 23. Appearance after cleaning (no brushes)

Figure 24. Appearance after cleaning (cleaning unit 1)

Figure 25. Appearance after cleaning (cleaning unit 2)

Figure 26. Appearance after cleaning (cleaning unit 3)

TABLE III. CLEANING RESULTS

	Diminution [g]	Cleaning performance [%]
Non-pile	7.5	12.2
Unit 1	12.5	21.9
Unit 2	20.5	35.7
Unit 3	37.5	60

VI. EXPERIMENT TO MEASURE BEST CLEANING PERFORMANCE

In the experiments of the previous section, we measured the cleaning performances of the developed cleaning units. Cleaning unit 3 had the best performance of 60.0%. Hence, in this section, we conduct a cleaning experiment using the developed robot with all the units configured as cleaning unit 3 (see Fig. 27). From the result, we can judge whether the cleaning performance (and therefore the effectiveness) of the developed robot is improved by increasing the number of cleaning units.

Figure 28 shows an experimental arrangement, which is the same as the pervious one except that now there are four cleaning units of type 3. In addition, each cleaning unit is displaced by a certain relative amount in the circumferential direction to avoid overlapping positions without brush between the cleaning units.

Figure 29 shows the appearance of the duct before and after cleaning. Table IV gives the diminution of the test powder and the cleaning performance. The latter is now 97.4%, which is 35.7 % higher than the best result of the previous section. Therefore, we have confirmed that increasing the number of cleaning units increases the cleaning

performance. We have also confirmed the cleaning performance is 97.4 %. On observing the robot after this experiment, we confirmed that the majority of test powder dislodged from the pipe was due to the leading unit, whereas the final unit cleaned those places that the front units had not cleaned. Thus, we think that the robot was able to clean more effectively by having brushes with a bigger contact area and better wiping action.

The aim now is to reach a cleaning performance of 99.8%. We also intend to investigate cleaning in an actual duct by conducting more cleaning experiments.

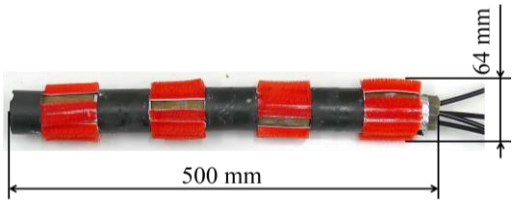

Figure 27. Appearance of the duct-cleaning robot

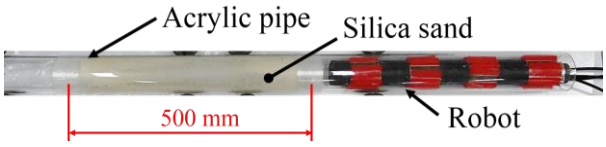

Figure 28. Experimental arrangement for duct cleaning

(a) Appearance before cleaning

(b) In the middle of cleaning 1

(c) In the middle of cleaning 2

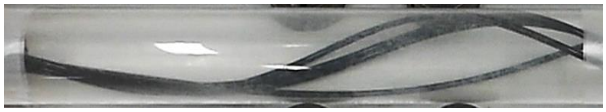

(b) Appearance after cleaning

Figure 29. Result of cleaning experiment using the robot

TABLE IV. RESULT OF CLEANING USING OPTIMIZED CLEANING UNITS

	Diminution [g]	Cleaning performance [%]
robot	56.5	97.4

VII. CONCLUSIONS AND FUTURE WORK

A. Conclusions

We have developed a cleaning unit to clean inside ducts and measured its maximum static friction force, extension and contraction characteristics, and cleaning performance. The maximum friction force exceeded the 72 N that was required for the robot to travel the target distance of 10 m. In addition, the necessary extension and contraction times to operate the robot were 0.9 s and 0.6 s, respectively. The maximum cleaning performance of the unit was 60.0% at first. However, after optimizing the cleaning configuration, this was improved to 97.4%. A desirable cleaning performance is 99.8 % in this paper's experiment. Hence, we aim to reach the figure.

B. Future works

- We intend to improve the cleaning performance by increase of scraping off force.
- We intend to develop a robot with flexible joints and use it to conduct cleaning experiments.

REFERENCES

[1] U.S. Environmental Protection Agency. 1990. Reducing risk: setting priorities and strategies for environmental protection. SAB-EC-90-021, Washington, DC.

[2] L. M. Brosseau, D. Vesley, T. H. Kuehn, J. Melson, and H. S. Han, "Dust cleaning: a review of associated health effects and results of company and expert surveys," *ASHRAE Trans*., No. 106, pp. 180–187, 2000.

[3] A. Seaton, J. Cherrie, M. Dennekamp, K. Donaldson, J. F. Hurley, and C. L. Tran, "The London Underground: dust and hazards to health," *Occupational & Environmental Medicine 2005*, Volume 62, Issue 6, pp. 354

[4] S. W. Jeon, W. Jeong, D. Park, and S. Kwon, "Design of an Intelligent Duct Cleaning Robot with Force Compliant Brush,"

[5] Osaka Winton Co., Ltd. Home Page. 16 Jan. 2017. Osaka Winton Co., Ltd. http://www.osaka-winton.co.jp/en/air_conditioning/

[6] A. Kuwada, K. Tsujino, K. Suzumori, and T. Kanda, "Intelligent actuators realizing snake –like small robot for pipe inspection," in 2006 Proc. IEEE International Symposium on Micro-nano Mechatronics and Human Science, pp. 1-6

[7] P. Li, S. Ma, B. Li, and Y. Wang, "Development of an adaptive mobile robot for in-pipe inspection task," in *Proc. IMCA International Conference on Mechatronics and Automation*, pp. 3622-3627, 2007

[8] M. Konyo, K. Hatazaki, K. Isaki, and S. Tadokoro, "Development of an active scope camera driven by ciliary vibration mechanism," *Proc. Of the 12th ROBOTICS symposia*, pp. 460-465, 2007

[9] H. Sugi, "Evolution of muscle motion," The University of Tokyo Press, p. 72, 1977 (in Japanese)

[10] T. Nakamura and H. Shinohama, "Position and Force Control Based on Mathematical Models of Pneumatic Artificial Muscles Reinforced by Straight Glass Fibers," in *Proc. IEEE International Conference on Robotics and Automation (ICRA 2007),* pp. 4361–4366.